

**U.S. DEPARTMENT OF COMMERCE
NATIONAL OCEANIC AND ATMOSPHERIC ADMINISTRATION
NATIONAL WEATHER SERVICE
OFFICE OF SCIENCE AND TECHNOLOGY INTEGRATION
METEOROLOGICAL DEVELOPMENT LABORATORY**

MDL OFFICE NOTE 20-1

**LAMP ALASKA CONVECTION AND LIGHTNING
VERIFICATION REPORT ***

**Jerome Charba, Phillip Shafer, Frederick Samplatsky, Andrew Kochenash,
and Judy Ghirardelli**

May 2020

*** Portions of work supported by the Joint Technology Transfer Initiative (JTTI) Program
within the NOAA/OAR Office of Water and Air Quality**

LAMP ALASKA CONVECTION AND LIGHTNING VERIFICATION REPORT

Jerome Charba, Phillip Shafer, Frederick Samplatsky, Andrew Kochenash, and
Judy Ghirardelli

1. INTRODUCTION

JTTI has funded the Meteorological Development Laboratory (MDL) to develop “Forecast Guidance for Aviation Tactical Operations and Strategic Planning over Alaska.” A component of this task is to extend Localized Aviation MOS Program (LAMP) convection and lightning (C-L) guidance for the CONUS (Charba et al. 2019) to the Alaska region. Specific C-L guidance products are forecast probability and potential. This report summarizes development and performance (verification) of the Alaska LAMP C-L probability and potential products.

The extension of CONUS C-L probability guidance to Alaska consists of developing and applying C-L probability regression equations to a rectangular Cartesian grid (12-km mesh) with National Blend of Models (NBM; Craven et al. 2020) Alaska geographical coverage (Fig. 1). Basic aspects of the Alaska C-L probability model are patterned after a similar model for the CONUS (Charba et al. 2019). However, to enhance model modularity, implementation flexibility, and consistency with recently-developed, JTTI funded LAMP Alaska ceiling and visibility (C-V) guidance (Schnapp et al. 2019), the Alaska C-L probability model has a somewhat different structure from that of the CONUS model.

A schematic illustration of the end-to-end Alaska C-L forecast guidance system is shown in Fig. 2, the brunt of which are three probability model components: Model Output Statistics (MOS), base-LAMP, and meld-LAMP (Glahn et al. 2017; Schnapp et al. 2019) probabilities. Note that the meld-LAMP comprises the end-product probability guidance, and the follow-on “potential” product is obtained through post-processing of the meld-LAMP C-L probabilities. It is important to mention early-on that development of Alaska C-L probabilities presented major unique challenges, particularly for convection. These challenges stem from the dearth of observational data over the Alaska region, especially radar data. Compensating for very poor radar coverage led to further challenges involving unexpected instabilities in the “compensating data.” Challenges that have caused substantial added effort in the development of the convection probability guidance are summarized next.

2. LAMP DEVELOPMENTAL CHALLENGES FOR ALASKA

The limited geographical coverage of radar data mentioned above is depicted in Fig. 1. Note that though Alaska NEXRAD “full coverage” is not especially small, i.e., the peak-range NEXRAD radar “umbrellas” cover 15.4% of the NBM grid domain, *usable* Multi-Radar Multi-Sensor (MRMS; Zhang et al. 2005; Langston et al. 2007; Smith et al. 2016) data cover just 2.0% (1.2%) of the NBM Alaska forecast domain for the warm season (cool season). This small effective radar coverage results from radar beam overshoot of precipitation and mountainous terrain occultation. Since composite reflectivity (CREF) has a dominant role in the convection

predictand specification (Charba et al. 2019), it was necessary to use surrogate (bogus) CREF observational data where MRMS CREF is not available or missing. A suitable surrogate CREF data source was considered to be 3-h CREF forecasts from the Rapid Refresh model (RAP; Benjamin et al. 2016). [Note that Charba et al. (2019) used 1-h forecasts from the High-Resolution Rapid Refresh Model (HRRR; Benjamin et al. 2016) for small CONUS areas of unusable MRMS data. Unfortunately, HRRR model data could not be used for Alaska because of inadequate HRRR geographical and temporal coverage (Schnapp et al. 2019).]

Compounding the challenge posed by limited Alaska radar coverage, the substitution of RAP CREF data resulted in added challenges: (1) since RAP model forecasts are used as a LAMP predictor input together with RAP CREF use in the convection predictand specification, an inherent, artificially-high correlation arises between RAP predictors and the convection predictand, and (2) RAP 3-h CREFs exhibit inter-cycle instability [the problem is even worse for 1- or 2-h RAP CREFs, the source of which may be twice-per-day adjustments in the RAP initialization scheme (see Benjamin et al. 2016)]. Addressing these challenges entailed extensive additional effort, which resulted in multiple delays in the development of RAP-based, base-LAMP, and meld-LAMP convection probabilities (Fig. 2). Still, the meld-LAMP Alaska convection (and lightning) probabilities ultimately developed have attractive forecast performance characteristics, as later sections of this report show.

3. DEVELOPMENT OF C-L PREDICTANDS, PREDICTORS, PROBABILITY, AND POTENTIAL

The development and production of the (final) meld-LAMP C-L probabilities consist of a three-step process (Fig. 2). Step 1 consists of the development and application of North American Mesoscale Model (NAM; Rogers et al. 2005)-based, European Centre for Medium-Range Weather Forecasting (ECM 2020)-based, and RAP-based MOS regression equations to produce MOS C-L probabilities. Step 2 uses NAM and ECM MOS probabilities from Step 1 as predictors together with observations-based (Obs) predictors to produce base-LAMP probabilities. Step 3 combines base-LAMP probabilities from Step 2 and RAP-MOS probabilities from Step 1 to obtain meld-LAMP probabilities. Note that the strategy underlying the meld-LAMP step is that it supports timely updates of “stable” base-LAMP probabilities with relatively frequent upgrades of high-resolution models, such as the RAP or HRRR (Glahn et al. 2017; Schnapp et al. 2019).

The development of all levels of C-L probabilities begins with specifying/defining the associated predictands. Defining characteristics of the Alaska C-L predictands (Table 1) are identical to corresponding CONUS C-L predictands (Charba et al. 2019), with notable exceptions. (1) For the lightning predictand and the lightning component of the convection predictand there is a switch from total lightning (TL) flashes to merged cloud-to-ground (CG) lightning return strokes [from three lightning observing systems (LLSs; Charba et al. 2020a,b)] for Alaska. This switch was necessitated by the non-existence of TL data for Alaska. (2) For the convection predictand (Table 1) there is a switch in the CREF criterion from ≥ 40 dBZ for the CONUS to ≥ 35 dBZ for Alaska; this was prompted by statistical analyses of CREF data, which showed ≥ 40 dBZ CREFs are relatively rare for Alaska. (3) For both lightning and convection there is an increase in the grid box size from 20 km for the CONUS to 24 km for Alaska, a

decision partially prompted by the relative rarity of C-L events for Alaska, particularly for lightning during the cool season of the year (increasing the box size increases the predictand event relative frequency). While these changes in the predictand definitions disallow strict comparisons of performance of CONUS and Alaska C-L forecast guidance, they may not be significant to many users.

Note that the CREF criterion in the convection predictand specification (Table 1) is more important than the lightning criterion because the frequency of ≥ 35 dBZ CREF is much higher than the frequency of ≥ 1 cloud-to-ground (CG) lightning return strokes. Also, since CREF data for the vast portion of the Alaska NBM grid area consists of RAP 3-h CREF forecasts, the convection predictand is dominated by these RAP forecasts. Thus, the validity of the convection predictand is highly dependent on the performance of RAP CREF forecasts. Since the LAMP convection probability guidance is developed with this predictand, the forecast performance of LAMP over most of the NBM grid area will inherently be strongly controlled by the performance of RAP CREF forecasts. The authors are not aware of previous investigations of the performance of RAP CREF forecasts over Alaska, nor have we conducted such an investigation in this work. On the other hand, during the convection predictor and predictand specifications we inadvertently discovered cycle-to-cycle instability in short range RAP forecasts. This RAP instability was a major obstacle in the LAMP convection probability development, and its nature and mitigation for LAMP convection probability development is discussed later in this section.

The Alaska LAMP model produces hourly-updated C-L probabilities in 1-h increments in the 1-38 h range throughout the year for the NBM grid (Fig. 1). The end-product meld-LAMP probabilities are produced with Obs and MOS-probability predictors summarized in Table 2. It is shown later in this section that Obs predictors have a dominant predictive role in the first few LAMP forecast projections, which is especially true for lightning, since the lightning predictors and predictand are very similarly defined. Still, the lightning predictors in Table 2 employ data from just one (GLD360) of three LLSs used in the (overall) Alaska LAMP probability development, as GLD360 are the only Alaska lightning data available for use in real time. Note also from Table 2 that an important property of the Obs predictors is their specification in two forms: (a) the current observation¹, which is used only for the LAMP 1-h forecast projection, and (b) the advected (current) observation, which is produced via a simple advection model (Glahn and Unger 1986; Charba et al. 2019) and applied to LAMP C-L predictands in the 1-8 h forecast range. Concerning the MOS probability predictors in Table 2, note that underlying each is a broad assortment of model-output predictors, which are meteorologically related to the lightning or convection predictand. For lightning, these predictors include various convective instability indices and moisture variables, which are physically related to thunderstorms, and for convection model-based moisture predictors were expanded and MRMS and RAP-simulated CREF predictors were added. Finally, a feature unique to RAP MOS C-L probabilities (Table 2; Fig. 2) is that each of the underlying RAP model predictors is specified as a weighted average of the most current RAP cycle and two earlier cycles, a technique currently in use for producing HRRR-based MOS 1-h precipitation probabilities (see Shafer et al. 2020). The rationale for the

¹ In the case of CREF, where the MRMS observation is missing, a RAP 3-h forecast is substituted (see Table 2)

RAP-predictor cycle-averaging strategy is to mitigate cycle-to-cycle inconsistencies in the RAP MOS probabilities, and ultimately in meld-LAMP C-L probabilities (Fig. 2).

Another important LAMP attribute underlying all levels of C-L probabilities is geographical stratification (regionalization) of the underlying regression equations. This entails developing separate regional equations for Alaska “land” and “water” areas for lightning (Fig. 3); for convection a third (MRMS) region is defined, which encompasses a relatively small area with MRMS data coverage. Note that probability regression equations for the MRMS region are expected to be relatively immune to the adverse impacts associated with the RAP CREF data substitution noted in section 2. Thus, convection probabilities for the MRMS region provide a quality benchmark for convection probabilities for neighboring land and water regions. Note also that adjacent lightning and convection regions slightly overlap (Fig. 3), which is necessary to avoid artificial discontinuities in C-L probability and potential products along region boundaries (Charba et al. 2019).

Further LAMP regression-equation stratifications are designed to capture climatologically-strong seasonal and diurnal variations of Alaska lightning and convection occurrences. This involves developing separate equations for (slightly-overlapping) warm (April 16 – October 15) and cool (August 16 - June 15) seasons, as well for each of 24 LAMP hourly cycles. Such stratifications help capture strong Alaska seasonal and diurnal lightning variability (Charba et al. 2020a) and thus in LAMP lightning guidance. For consistency, this stratification is also applied for convection, even as convection seasonal and diurnal variabilities are much weaker than for lightning.

Since most Alaska lightning events occur in June and July (Charba et al. 2020a) and very little lightning occurs during October- April, the development of statistically-stable, skillful lightning probability regression equations posed a challenge, particularly for the cool season. Fortunately, a relatively-long, stable historical sample (April 2013 – October 2019) was available to support development of lightning (predictand) monthly relative frequencies (MRFs; i.e., lightning climatology) for every month of the year and every hour of the day. Note that that MRFs are used as a predictor (Table 2), and in the next section evidence is shown to indicate that lightning MRFs contribute appreciably to lightning probability skill. Meanwhile, the starting date for samples used specifically for development of meld-LAMP C-L probability regression equations is more recent, i.e., 08 May 2016, as this is when archived RAP CREF is first available. Note also that since archived MRMS CREF observations do not begin until 01 September 2016, RAP-forecasted CREF data were used exclusively for LAMP development dating backward to 08 May 2016. Since the LAMP developmental sample then extends forward to 31 October 2019, the meld-LAMP C-L warm season (cool season) regression equations are based on four (three) seasons of data, which is rather short for the rare-event C-L predictands.

Finally, adverse impacts (and ensuing treatments) arising from RAP CREF use in LAMP bears stressing. Since RAP-forecasted CREF is used in both the convection predictand and RAP-MOS predictor specifications, (as mentioned earlier) an artificially-high predictor-predictand correlation inherently arises in the RAP-MOS convection probability regression equations, especially involving the land and water regions (Fig. 3) for the 1-6 h forecast range. Without treatment, this results in fictitiously-high “skill” (and sharpness) in the RAP MOS

convection probabilities (and ultimately in the meld-LAMP convection probabilities). The problem was treated (for the 1-12 h forecast range) via stepwise extensions of the RAP three-cycle predictor-averaging technique discussed above (RAP cycles as old as 12 hours were used in the 1-6 h range). This extension of the three-cycle predictor-averaging technique effectively suppressed the artificially-high LAMP convection probability skill and sharpness, as noted in the subsequent section.

As shown in Fig. 2, meld-LAMP C-L “potential” is derived from the corresponding probabilities. [Charba et al. \(2019\)](#) recently introduced convection and lightning potential, which they derived from and applied to LAMP lightning and convection probability for the CONUS. Note that while the development algorithm for potential has the capability to yield any number of predictand-event threat categories, two is the minimum, i.e., the predicted event occurrence and non-occurrence (yes/no forecasts). In the application of the method to C-L probabilities, [Charba et al. \(2019\)](#) specified four threat categories, namely “no”, “low”, “medium”, and “high”, where the forecast bias associated with each is prescribed (and therefore known) within a very narrow range. Also, when the no and low categories are aggregated and then redefined as no and aggregated medium and high categories are similarly redefined as yes, the threat score (same as the critical success index; see [Schaefer 1990](#)) for these new no/yes forecasts is maximized and the bias is generally in the 1.0 -1.3 range (slight over forecasting, as unbiased forecasts have a 1.0 value). The reader is referred to [Charba et al. \(2019\)](#) for detailed information on the development of potential.

4. VERIFICATION OF C-L PROBABILITY AND POTENTIAL

C-L probability and potential forecasts have been developed and validated for the full Alaska LAMP domain. Validation consists of verifying with the developmental sample and examining performance statistics to ensure correctness of the forecasts and to understand forecast characteristics. In addition, the performance of C-L probability and potential forecasts was tested for the 00- and 12-UTC LAMP cycles using June-July (warm season) and November-December (cool season) 2017 independent samples. Selected examples of C-L verification statistics are discussed here (lightning first, as the lightning verification is less complex than for convection).

A. Lightning Probability

The forecast performance of C-L probabilities was measured with the Brier Skill Score (BSS; [Wilks 2006](#)), where the predictand MRF (Table 2) was used as a no skill reference. Note that since BSSs based on the developmental sample were produced for all 24 LAMP hourly cycles, these are used to aid interpretation of corresponding independent-sample BSSs for the 00- and 12-UTC cycles. A secondary skill benchmark used in this study involves persisting the current observation of a key LAMP Obs predictor (Persistence) over all LAMP forecast projections. For lightning, Persistence is defined as the yes/no occurrence of ≥ 1 GLD360 CG strokes (over 30 minutes) ending at hh:15, where hh is the LAMP cycle time (clock hour). This Persistence measure is appropriate, since the parameter is available in real time and therefore used as a critical lightning predictor (Table 1; 2).

For lightning, verification is shown only for the 12-UTC LAMP cycle since the verification for other cycles is little different. Figure 4 indicates quite high meld-LAMP “skill”² at the first (1-h) forecast projection, but skill then drops very sharply to 3 hours, and afterward it is relatively flat at a rather low level across all longer projections. Relatively high skill at the first hourly projection is a signature characteristic of LAMP (Ghirardelli et al. 2010; Glahn et al. 2017); it reflects the high effectiveness of Obs predictors, which is implied by the LAMP (meld and base) and MOS (NAM-, ECM-, and RAP-based) curves in Fig. 4. The rate of skill fall afterward varies among LAMP aviation forecast elements, and for Alaska lightning the fall rate is extreme – higher than for CONUS lightning (Charba et al. 2019). Figure 4 indicates this extreme skill fall-off is due to rather small skill contributions from NAM-, ECM-, and RAP-based MOS probabilities. Further, since base-LAMP skill is almost as high as for meld-LAMP, the RAP-MOS skill contribution is very small – smaller than the HRRR skill contribution to CONUS LAMP lightning probabilities (Charba et al. 2019). Note that Alaska Persistence skill is fairly close to meld skill at the first projection, but it “exponentially” drops to negative skill beyond 2-3 hours (and therefore not plotted in Fig. 4).

Regionally, Fig. 4 shows much higher lightning skill for the land region compared to the water region, especially for projections beyond 6 hours. This feature is consistent with Obs predictor dominance for the early projections, and perhaps also that GLD360 lightning detection efficiency is weaker (at least in past years) over the north Pacific than over Alaska (thus relatively weak lightning Obs predictors for the water region) and weak MOS skill contributions for longer projections (noted above). Also, the land region exhibits a clear diurnal cycle in skill, which suggests an appreciable skill contribution from the lightning predictand MRF (Table 2). It is worth noting that lightning BSS characteristics (based on the developmental sample) for all other LAMP cycles (not shown) are quite similar to those in Fig. 4 -- the main difference is the phase of the diurnal skill cycle.

Figure 5 shows lightning BSS for the June-July 2017 (warm season) test sample. Note that even though this sample is rather short, the BSS curve for land (Fig. 5a) well matches the corresponding curve for the much longer developmental sample (Fig. 4c), and this also applies for the water region (Fig. 5b versus Fig. 4d). Increased BSS fluctuations versus projection in Fig. 5 are due to the shortness of the test sample, which is especially evident for the water region (Fig. 5b). Corresponding test sample curves for the cool season are not shown, as they were found essentially meaningless because of very few lightning occurrences. Also, test-sample BSS curves for the 00-UTC cycle (not shown) are similar to those for 12 UTC.

B. Convection Probability

For convection, the BSS is computed in the same way as for lightning. Convection Persistence is defined using the most recent yes/no occurrence of CREF ≥ 30 dBZ (MRMS

² This skill indication is approximate at best, since the developmental sample is used. Still, it may be a better indicator of true (long term) skill than with the test sample, since the latter is short and Alaska lightning occurrences are rare events. Note that Alaska lightning frequency is quite low during the non-convective portion of the day, in the cool season, and anytime in the water region (Charba et al. 2020a).

observed and/or RAP forecasted). While this Persistence specification does not include lightning (as in the convection predictand specification), it still provides a useful persistence skill benchmark since Alaska CREF ≥ 30 dBZ events are far more common than Alaska lightning events, particularly for the cool season and/or the convectively-stable part of the day. Also, as for lightning, the verification statistics for the relatively long developmental sample are discussed first since they are more stable than those for the short independent (test) samples.

Verification characteristics for convection probability are diverse and complex, especially across the three convection regions (Fig. 3). Figure 6 shows convection probability BSS versus projection plots by region for the 12-UTC LAMP cycle during the cool season, and Fig. 7 contains corresponding plots for the warm season. All meld- and base-LAMP BSS curves in Figs. 6-7 show high skill at the first projection followed by a substantial skill decrease with subsequent projections. This contrasts with a very steep corresponding skill fall-off for lightning (Fig. 4), as convection shows a more gradual skill decline with time, especially for the land and water regions. Figures 6 and 7 both indicate that the weaker convection skill fall-off, especially for the land and water regions, is due to the inherently-high correlation between RAP predictors and the “RAP-contaminated” convection predictand (section 2). Specifically, note that RAP MOS skill matches meld skill in the 3-12 h projection range in the land and water regions for both the cool (Fig. 6) and the warm (Fig. 7) season. Contrastingly, for the MRMS region, where the inherent correlation is expected to be weaker, these figures show a more rapid meld skill fall-off, which is more similar to that for lightning. Note also, that base-LAMP skill, especially in the 3-12 h range, is much lower than meld skill for the land and water regions, whereas for the MRMS region base-LAMP skill is just slightly lower than meld skill. Further, RAP MOS skill for the MRMS region is substantially lower than meld skill for all forecast projections. The essential point here is that some portion of RAP MOS (and thus meld) convection “skill”, particularly for the land and water regions, is fictitious. As discussed in section 2, the underlying cause of this problem is the dearth of MRMS CREF data over the Alaska region. Finally, in Figs. 6-7 Persistence shows positive skill out to just 3-4 hours for the MRMS region; for the land region Persistence skill is even weaker, and for the water region Persistence skill is essentially negligible. These Persistence skill characteristics are consistent with those for lightning.

It is important to point out that we developed and incorporated a technique to mitigate the high internal correlation between RAP predictors and the “RAP-contaminated” convection predictand, and the RAP MOS and meld-LAMP BSS curves in Figs. 6-7 incorporate the mitigation. The technique involves averaging RAP predictors across three RAP cycles: the most current cycle and two earlier ones. The earlier cycle times vary stepwise as a function of LAMP forecast projection, where the earliest is 12, 6, and 3 hours old for the 1-6, 7-12, and beyond-12-h projection range, respectively. This technique strongly reduced (“mitigated”) very-high BSS scores (particularly for short forecast projections) due to the inherently-high correlation (not shown), but it did not fully remove the problem, as Figs. 6-7 show.

It is also important to note that the LAMP benefits from the RAP predictor-averaging technique vary across the 24 LAMP cycles. Specifically, the technique worked well for the 10-12 and 22-00 UTC cycle ranges, but it performed progressively more poorly for intervening cycles, where the worst performance is for 06- and 18-UTC cycles. The underlying reason for the RAP-cycle dependency appears to be a twice-per-day adjustment (for the 09- and 21-UTC

RAP cycles) in the model initialization scheme (see [Benjamin et al. 2016, pages 1672-1674](#)), which results in a corresponding “reset” in statistical properties of short range (~1-6 h) RAP forecasts. While the RAP predictor-averaging technique effectively mitigated the high internal predictor-predictand correlation, it did not remove (for most cycles) an adverse impact of this “reset” on RAP MOS and meld-LAMP convection probabilities. Figure 8 shows the adverse impact for the 18-UTC cycle (one of two cycles with peak adverse impact noted above). Note the unrealistic discontinuous BSS drop-off across the 5-6 h forecast projections for RAP MOS and meld-LAMP, which is strong for the land and water regions and weak for the MRMS region. Though these (regionally-dependent) skill drop-offs are concerning, our inspection of selected meld forecast probability maps has not revealed evidence of its potential adverse impact for the MRMS region. For the land and water region, the skill drop-off is reflected as a clear probability sharpness ([Wilks 2006](#)) drop-off (not shown), which may be noticed by users.

Seasonal skill variations for convection are minor, especially in comparison to those for lightning. That is, Fig. 6 shows somewhat higher convection skill during the cool season compared to the warm season (Fig. 7). Also, convection shows little or no evidence of a diurnal cycle in probability skill. These skill characteristics contrast with those for lightning, as the latter shows higher skill during the warm season than the cool season and a clear diurnal cycle, even for the cool season (Fig. 4).

Convection BSS charts for the test sample are shown in Fig. 9 (cool season) and Fig. 10 (warm season) for the 12-UTC LAMP cycle. Comparing against the corresponding developmental-sample charts [Fig. 6 (cool season) and Fig. 7 (warm season)], we find that broad BSS characteristics for the test sample are quite similar to those of the developmental sample for the cool season; for the warm season test sample skill (Fig. 10) is generally slightly lower than for the cool season (Fig. 7). Also, the test sample curves exhibit increased random BSS fluctuations with projection and diurnal BSS variations for the warm season, neither of which exist for the developmental sample. These skill departures for the test samples are not surprising considering shortness of the latter.

C. Example C-L Probability Maps

Example meld-LAMP lightning probability maps together with observed CG stroke counts (merged from the three LLSs noted in section 3) are shown in Fig. 11 for an intense warm season Alaska lightning event that occurred 08 July 2017. Note that for the 1-h projection, the probabilities are tightly focused spatially and very sharp (mostly close to either 0 % or 100 %), and the match with observed lightning strokes is quite good. This finding is consistent with very high lightning BSS for the 1-h projection in Figs. 4 and 5. For the 24-h projection, the probability pattern is smeared (spatially), the sharpness is much weaker, and the match with observed lightning is also weaker, which altogether is consistent with rather low lightning BSS for this longer LAMP forecast projection.

Corresponding meld-LAMP convection probability maps are shown in Fig. 12 for a cool season case of widespread convection that occurred 26 November 2017. For the 1-h projection, the convection probability map characteristics are similar to those for lightning in Fig. 11, where the main departures are expanded coverages of 100 % probability and observed convection. For

the 24-h projection, we see reduced areal focus and sharpness of the probabilities (expected), but still spatial focus and peak probabilities are higher than for lightning. These findings are consistent with corresponding convection probability BSSs in Figs. 6 and 9, which show less skill fall-off with increasing projection than for lightning (Figs. 4 and 5).

D. C-L Potential: Example Maps and Verification Statistics

LAMP potential, which is derived from LAMP probability, was briefly discussed in section 3. As discussed by [Charba et al. \(2019\)](#), LAMP potential has attributes that can strongly aid use of the associated probabilities, especially where the probability skill and sharpness ([Wilks 2006](#)) vary strongly as a function of forecast projection, time of the day, season, and geographical region. The Alaska C-L probabilities exhibit such skill and sharpness variability -- for lightning the variability is extreme.

Figure 13 shows maps of meld-LAMP lightning potential together with maps of the verifying lightning observations for comparison to corresponding lightning probability maps in Fig. 11. Figure 13 shows good consistency, from the 1-h projection to the 24-h projection, in the forecasted threat categories and areal coverage, which contrasts with corresponding extreme reduction in peak probabilities in Fig. 11. Since extensive lightning occurred for both valid times in this case, it indicates potential can aid interpretation of the probabilities, especially for typical LAMP situations of lower peak probabilities at the longer forecast projections. For the cool season convection case at hand, Figure 14 shows convection potential and verifying observation maps for these same forecast projections for comparison to corresponding convection probability maps in Fig. 12. As for the lightning example, this convection case shows strongly decreasing peak probabilities with increasing projection while the potential forecast is more consistent with extensive observed convection that continued at the longer forecast projection. The essential point is that LAMP probabilities typically decrease with increasing forecast projection, whereas the areal coverage and event threat categories for potential are usually more consistent with the verifying observations.

Threat score (TS; over the full NBM grid area) versus forecast projection (verification) charts for meld-LAMP lightning and convection potential are shown in Fig. 15 for the developmental and test samples, the warm season, and the 12-UTC cycle. Each chart in the figure contains a TS curve for low and above, medium and above, and high potential, respectively denoted LOW, MED, and HIGH in the legend. First, note that shapes of these warm season TS curves are similar to the corresponding (regionalized) BSS curves for both lightning and convection [Figs. 4c (land region) and 5a (land region) for lightning and Figs. 7 (all regions) and 10a and 10b (MRMS and land regions)]. The increased TS-BSS similarity for the land region versus the water region likely reflects much higher frequency of lightning and convection for land versus water areas during the warm (convective) season. Note also in Fig. 15 that the TS for high potential (HIGH) is generally lower than for low and above (LOW) and medium and above (MED) potential, which is consistent with the relatively low frequency of high potential (equivalent to relatively low areal coverage of high potential in individual potential forecast maps, as shown in Figs. 13 and 14).

Figure 16 shows an example of forecast bias (ratio of forecasted to observed events) characteristics for the LOW, MED, and HIGH potential categories. Note the strong over-forecasting for LOW, very slight over-forecasting for MED, and strong under-forecasting for HIGH, each of which is remarkably consistent across all forecast projections. Specifically, the bias curves in this figure are for the same sample as for the corresponding TS curves in Fig. 15a, and yet the bias curves show no evidence of the strong diurnal variation seen in the TS curves. These are signature bias characteristics of potential, as they are inherent to its specification (Charba et al. 2019). Of course, significant deviations from this example can occur with small verification samples, which is the case in this study for the cool season lightning test samples (not shown).

5. SUMMARY, COMMENTS, AND PLANS

The development and performance of LAMP lightning and convection probability guidance for the NBM Alaska grid is described. For lightning, the probability development proceeded relatively smoothly and on-schedule, despite extra effort associated with applying lightning data from three lightning locating systems. The extreme seasonal variability of Alaska lightning posed minor development challenges, as lightning is largely limited to the afternoon and evening of the warm season. Alaska lightning probabilities are quite skillful for the first few hours following their hourly issuance due to high predictive power of extrapolated lightning observations. Conversely, their skill for longer forecast projections is rather low, which suggests weak lightning predictive utility of NAM, ECM, and RAP model output.

The development of Alaska LAMP convection probabilities was rather difficult and fraught with obstacles stemming from the dearth of Alaska radar reflectivity data. The substitution of RAP-simulated reflectivity for unavailable MRMS observations allowed development of the convection probabilities, but multiple ensuing technical obstacles were encountered. Addressing these challenges and mitigating their adverse impacts appear largely successful, particularly for the (limited) Alaska region with partial radar coverage. The skill of the LAMP convection probabilities appears strong for this region, even for projections beyond the predictive range of current observational data. For the remainder of the Alaska forecast area, the convection probability skill is largely indeterminant because of incomplete convection ground truth data there. On the other hand, the convection probability performance characteristics appear mostly consistent across the entire NBM Alaska grid area. From this perspective, the convection probabilities may provide useful guidance throughout the NBM grid area.

Attractive attributes of LAMP C-L potential guidance were discussed and demonstrated. Since forecast bias associated with each of the four potential (predictand event threat) categories is inherently known, potential can uniquely aid use of the probabilities, especially where the skill and sharpness of the probabilities vary greatly as a function of forecast projection, geographical location, time of the day, day of the year, etc. Large variability in these probability characteristics is especially true of the Alaska lightning probabilities. Forecast accuracy of LAMP potential is inherently linked to LAMP probability skill, since potential is derived from the probabilities.

To date we have completed development of the C-L probability regression equations and probability thresholds needed for producing the C-L probability and potential guidance in real time. We plan real time production of this “experimental” guidance on NOAA's Weather and Climate Operational Supercomputing System (WCOS) around mid-May 2020. Guidance graphics will be available to restricted users by the early summer 2020 to evaluate LAMP forecast and system performance. By late summer the evaluation will be completed, and if favorable the Alaska LAMP system will immediately be submitted for implementation on WCOS.

REFERENCES

- Benjamin, S. G., and Coauthors, 2016: A North American hourly assimilation and model forecast cycle: The Rapid Refresh. *Mon. Wea. Rev.*, **144**, 1669–1694, <https://doi.org/10.1175/MWR-D-15-0242.1>.
- Charba, J. P., F. G. Samplatsky, A. J. Kochenash, P. E. Shafer, J. E. Ghirardelli, and C. Huang, 2019: LAMP upgraded convection and total lightning probability and “potential” guidance for the conterminous United States. *Wea. Forecasting*, **34**, 1519–1545, <https://journals.ametsoc.org/doi/pdf/10.1175/WAF-D-19-0015.1>.
- , —, —, —, and —, 2020a: Climatological properties of reported cloud-to-ground lightning for Alaska from several lightning detection systems. *20th Conference on Aviation, Range, and Aerospace Meteorology*, Boston, MA, Amer. Meteor. Soc., **363440**, <https://ams.confex.com/ams/2020Annual/webprogram/Paper363440.html>.
- , —, —, —, and —, 2020b: Development of LAMP convection and cloud-to-ground lightning forecast guidance for Alaska and beyond. *20th Conference on Aviation, Range, and Aerospace Meteorology*, Boston, MA, Amer. Meteor. Soc., **J42.3**, <https://ams.confex.com/ams/2020Annual/webprogram/Paper364031.html>.
- Craven, J.P., D.E. Rudack, and P.E. Shafer, 2020: National Blend of Models: A statistically post-processed multi-model ensemble. *J. Operational Meteor.*, **8** (1), 1–14, doi: <https://doi.org/10.1519/nwajom.2020.0801>.
- ECM, 2020: “European Centre for Medium-Range Weather Forecasts is an independent intergovernmental organization supported by 34 (member)states,” <https://www.ecmwf.int/en/forecasts>.
- Ghirardelli, J.E. and B. Glahn, 2010: The Meteorological Development Laboratory’s aviation weather prediction system. *Wea. Forecasting*, **25**, 1027–1051, <https://doi.org/10.1175/2010WAF2222312.1>.
- Glahn, H. R., and D. A. Unger, 1986: A Local AFOS MOS Program (LAMP) and its application to wind prediction. *Mon. Wea. Rev.*, **114**, 1313–1329, [https://doi.org/10.1175/1520-0493\(1986\)114,1313:ALAMPA.2.0.CO;2](https://doi.org/10.1175/1520-0493(1986)114,1313:ALAMPA.2.0.CO;2).

- _____, B., A. D. Schnapp, J. E. Ghirardelli, and J.-S. Im, 2017: A LAMP-HRRR meld for improved aviation guidance. *Wea. Forecasting*, **32**, 391-405., <https://journals.ametsoc.org/doi/pdf/10.1175/WAF-D-16-0127.1>
- Langston, C., J. Zhang, and K. Howard, 2007: Four-dimensional dynamic radar mosaic. *J. Atmos. Oceanic Technol.*, **24**, 776-790, <https://journals.ametsoc.org/doi/pdf/10.1175/JTECH2001.1>.
- Rogers, E., and Coauthors, 2005: The NCEP North American Mesoscale Modeling System: Final Eta model/analysis changes and preliminary experiments using the WRF-NMM. *21st Conf. on Weather Analysis and Forecasting/17th Conf. on Numerical Weather Prediction*, Washington, DC, Amer. Meteor. Soc., **4B.5**, https://ams.confex.com/ams/WAFNWP34BC/techprogram/paper_94707.htm.
- Schaefer, T. J., 1990: The critical success index as an indicator of warning skill. *Wea. Forecasting*, **5**, 570–575, [https://doi.org/10.1175/1520-0434\(1990\)005<0570:TCSIAA.2.0.CO;2](https://doi.org/10.1175/1520-0434(1990)005<0570:TCSIAA.2.0.CO;2).
- Schnapp, A., J. Ghirardelli, and B. Glahn, 2019: LAMP Alaska ceiling and visibility meld verification report. MDL/CIRA Report to JTTI, 16 pages.
- Shafer, P. E., J. P. Charba, F. G. Samplatsky, 2020: Experimental LAMP 1-h probability of precipitation guidance for the CONUS in support of the National Weather Service's National Blend of Models. AMS 100th Annual Meeting, 10th Conference on Transition of Research to Operations, Amer. Meteor. Soc., Boston, MA., <https://ams.confex.com/ams/2020Annual/meetingapp.cgi/Paper/364315>.
- Smith, T. M., and Coauthors, 2016: Multi-Radar Multi-Sensor (MRMS) severe weather and aviation products. *Bull. Amer. Meteor. Soc.*, **97**, 1617–1630, <https://doi.org/10.1175/BAMS-D-14-00173.1>.
- Wilks, D. S., 2006: Statistical Methods in the Atmospheric Sciences. 2nd ed. International Geophysics Series, Vol. 100, Academic Press, 648 pp.
- Zhang, J., K. H. Howard, and J. J. Gourley, 2005: Constructing three-dimensional multiple-radar reflectivity mosaics: Examples of convective storms and stratiform rain echoes. *J. Atmos. Oceanic Technol.*, **22**, 30- 42, <https://journals.ametsoc.org/doi/pdf/10.1175/JTECH-1689.1>.

Table 1. Defining characteristics of the lightning and convection predictands [hh denotes LAMP-cycle clock hour (00 – 23 UTC)].

<u>Lightning</u>	
Weather criterion	≥ 1 cloud-to-ground (CG) lightning return strokes*
Area **	Square grid box 24 km on a side
Valid period	1 hour [(hh-1):00 – hh:00]
<u>Convection</u>	
Weather criteria	≥ 1 cloud-to-ground (CG) lightning return strokes ≥ 35 dBZ CREF
Area	Same as for lightning
Valid period	Same as for lightning

* Strokes are merged from three lightning locating systems (see text).

** Adjacent grid-box centers are spaced 12 km apart

Table 2. (a) Observational (Obs) and (b) Model Output Statistics (MOS) -based potential predictors for the C-L predictands. In (a) and (b) “predictand” refers to convection and/or lightning and in (a) hh denotes the LAMP model cycle time, where hh = 00, 01, ..., 23 UTC. Abbreviations in (a) are: max = maximum value in the 24-km predictand grid box; MRMS = Multi-Radar Multi-Sensor system; CREF = composite radar reflectivity.

(a) Obs ^a
MRMS-RAP ^b max CREF
60-min CG stroke count ^c ending at hh:15
30-min CG stroke count ending at hh:15
30-min CG stroke count ending at hh:15 – 30 min CG stroke count ending at (hh-1):45
Predictand monthly relative frequency (MRF)
(b) MOS ^d
Model ^e -based predictand probability
Model ₁ -based predictand probability x model ₂ -based predictand probability ^f
Model-based predictand probability x predictand monthly relative frequency
Model-based predictand probability x terrain elevation

^a Obs predictors are comprised of two forms of the listed variables: (i) the current observation, and (ii) the advected (current) observation

^b MRMS-RAP denotes a composite of the current MRMS observation and a RAP 3-h forecast, where the former is valid at hh:14 and the latter at hh:00. This predictor was not used for base-LAMP lightning probability regression equations due to the relative shortness of MRMS and RAP historical archives (see text).

^c CG stroke count is from GLD360 observations

^d Underlying each MOS probability is a broad assortment of model output predictors, where each is physically related to the predictand (see text).

^e Model denotes North American Mesoscale (NAM), European Centre for Medium Range Forecasting (ECM), and Rapid Refresh (RAP).

^f Model₁ denotes NAM; model₂ denotes ECM

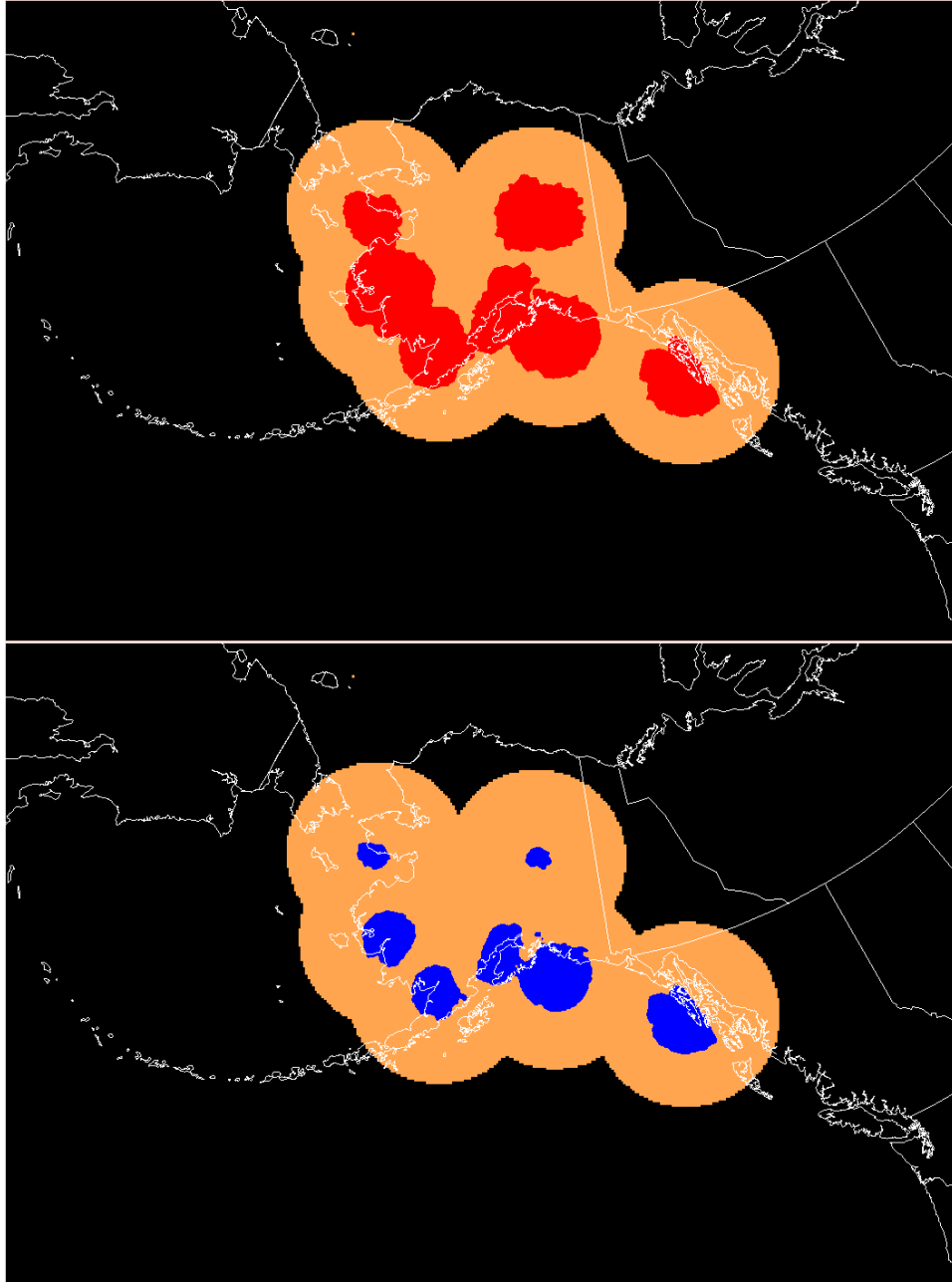


Figure 1. National Blend of Models (NBM) Alaska grid coverage (black), NEXRAD radar coverage (light orange), and usable MRMS data coverage during the warm season (top) and cool season (bottom).

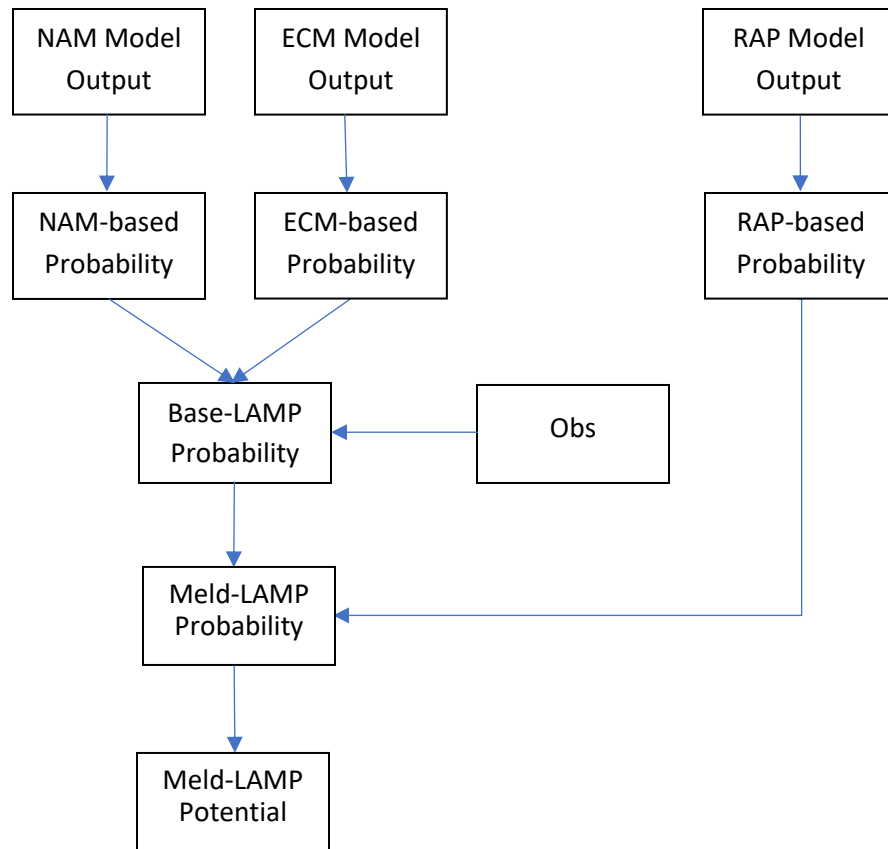


Figure 2. Schematic flow diagram for Alaska meld-LAMP convection and lightning probability and "potential" guidance. See text and Table 1 for acronyms and abbreviations.

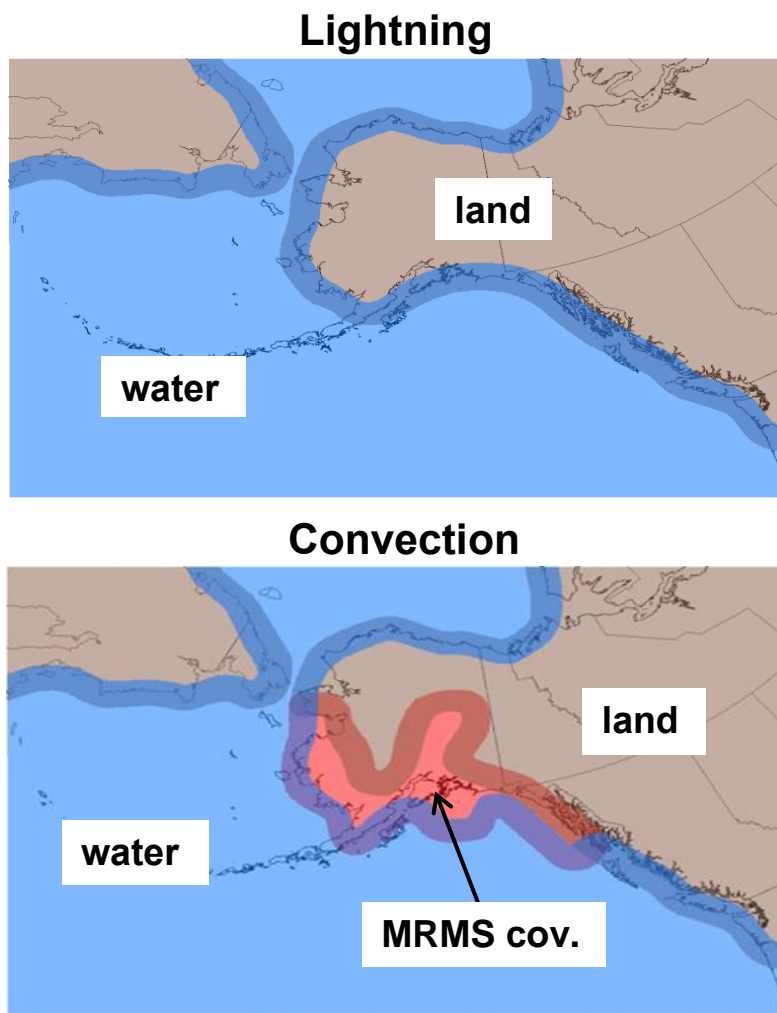


Figure 3. Lightning and convection regions. Slight overlap of adjoining regions is indicated by the blended color shades.

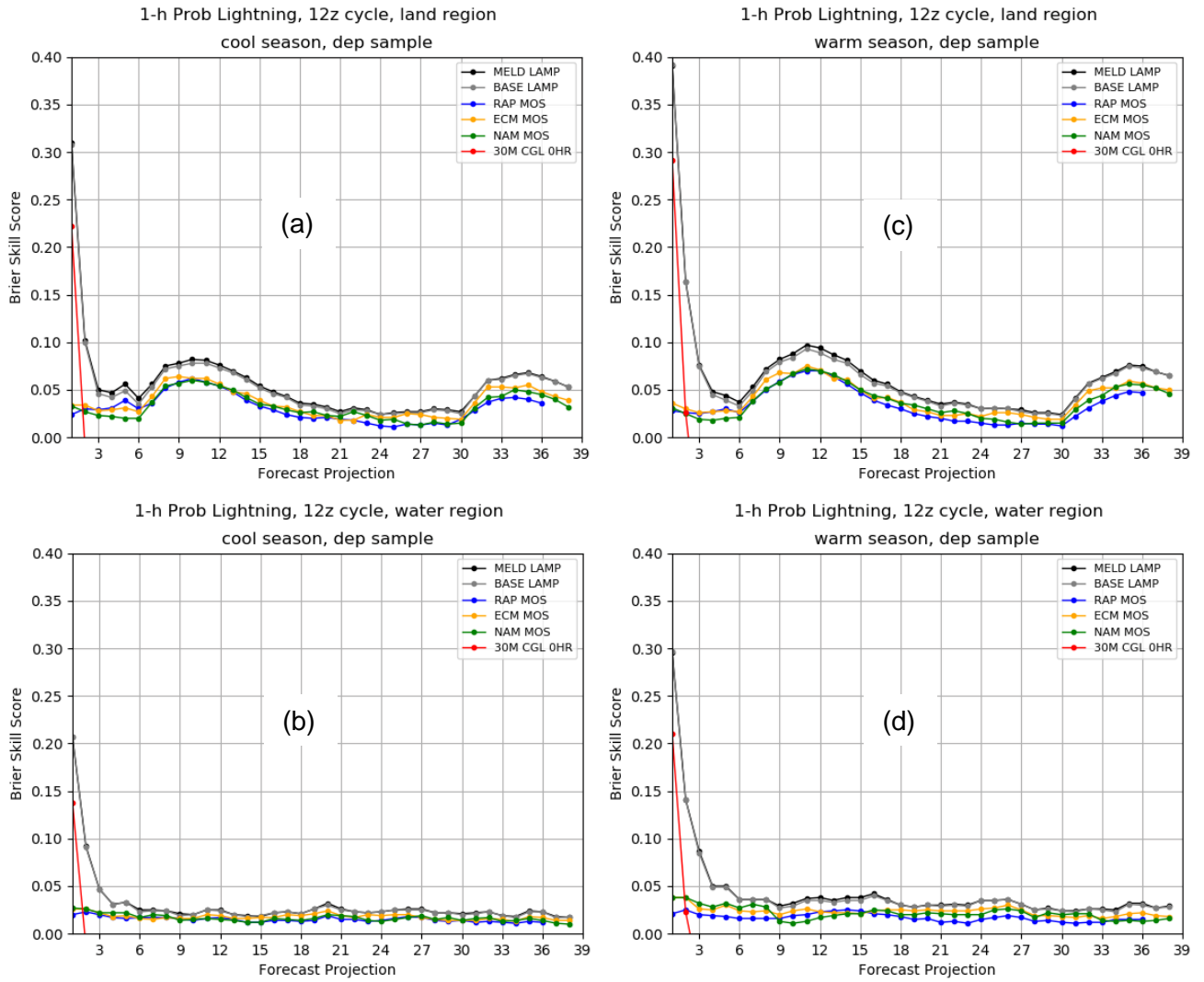


Figure 4. Lightning probability Brier Skill Score (BSS, decimal unit) for the developmental sample and the 12-UTC LAMP cycle of the cool season, where (a) is for the land region and (b) is for the water region (Fig 3). Corresponding BSS charts are also shown for the warm season, where (c) is for the land region and (d) is for the water region. The unit for “Forecast Projection” (abscissa label) is hours. Legend: “30M CGL 0HR” denotes Persistence (see text); values beyond two hours are negative (not shown); see text for other legend items. In the titles, Prob denotes probability, z denotes UTC, and dep denotes developmental (dependent) sample.

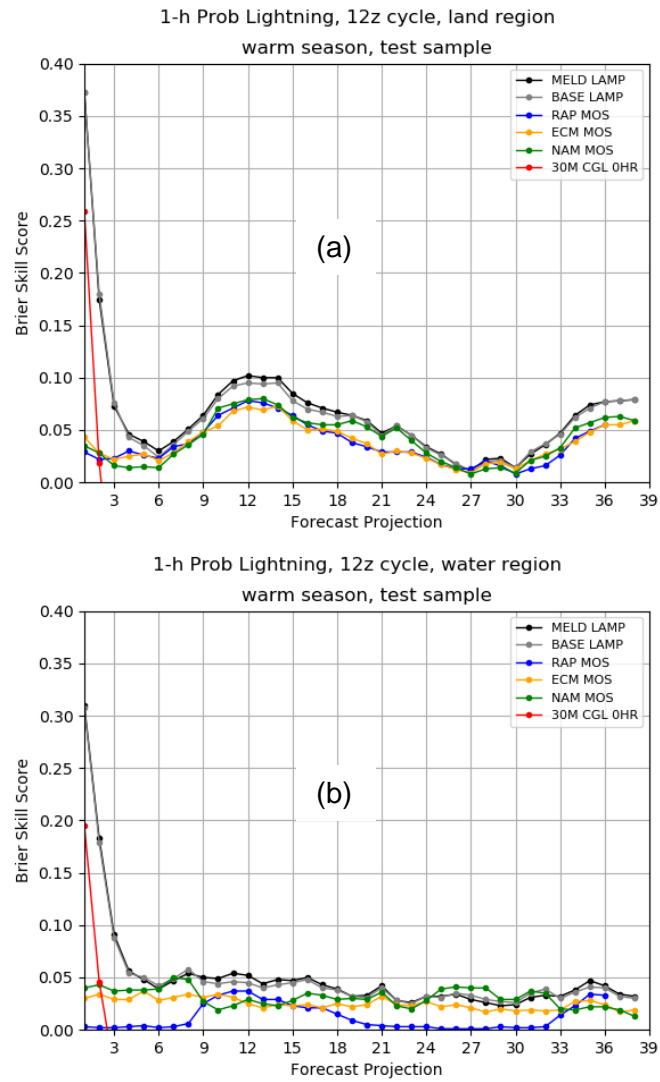


Figure 5. (a) As for Fig. 4c and (b) as for Fig. 4d, except for the June-July 2017 test (independent) sample.

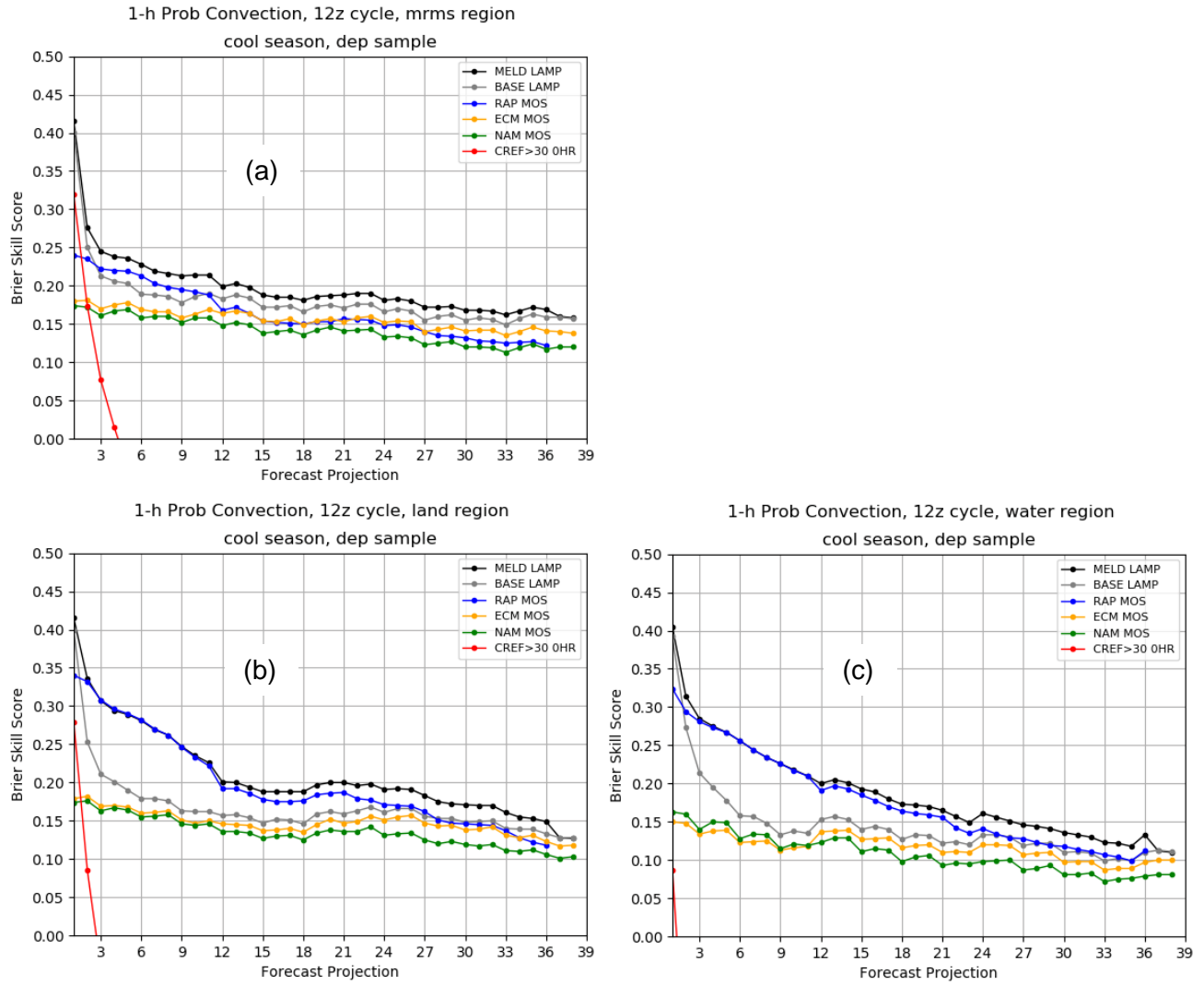


Figure 6. As in Figure 4, except for convection during the cool season, where (a) is for the MRMS, (b) land, and (c) water region (Fig. 3). Legend: “CREF > 30 0HR” denotes Persistence (see text).

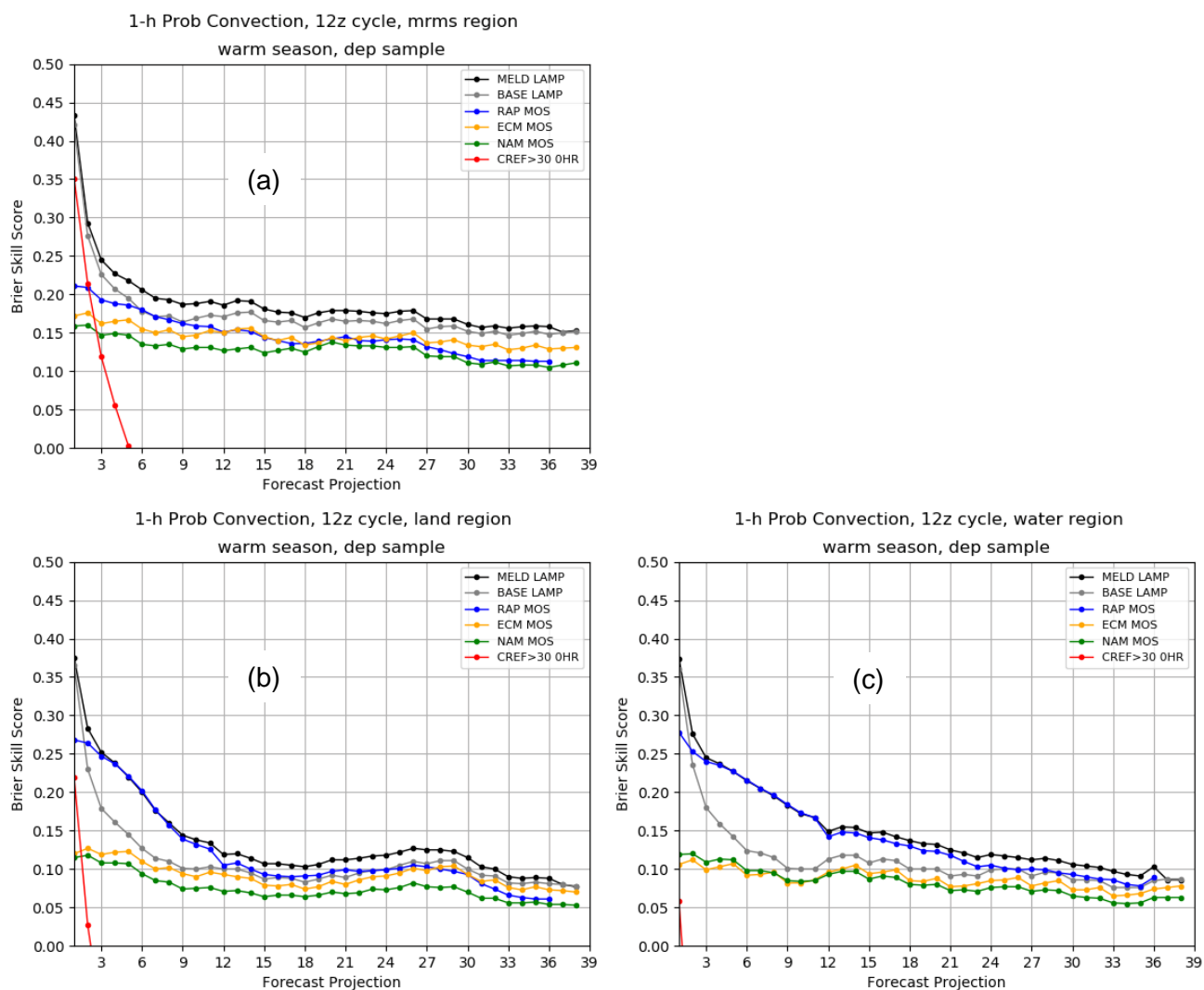


Figure 7. As in Figure 6 for the warm season.

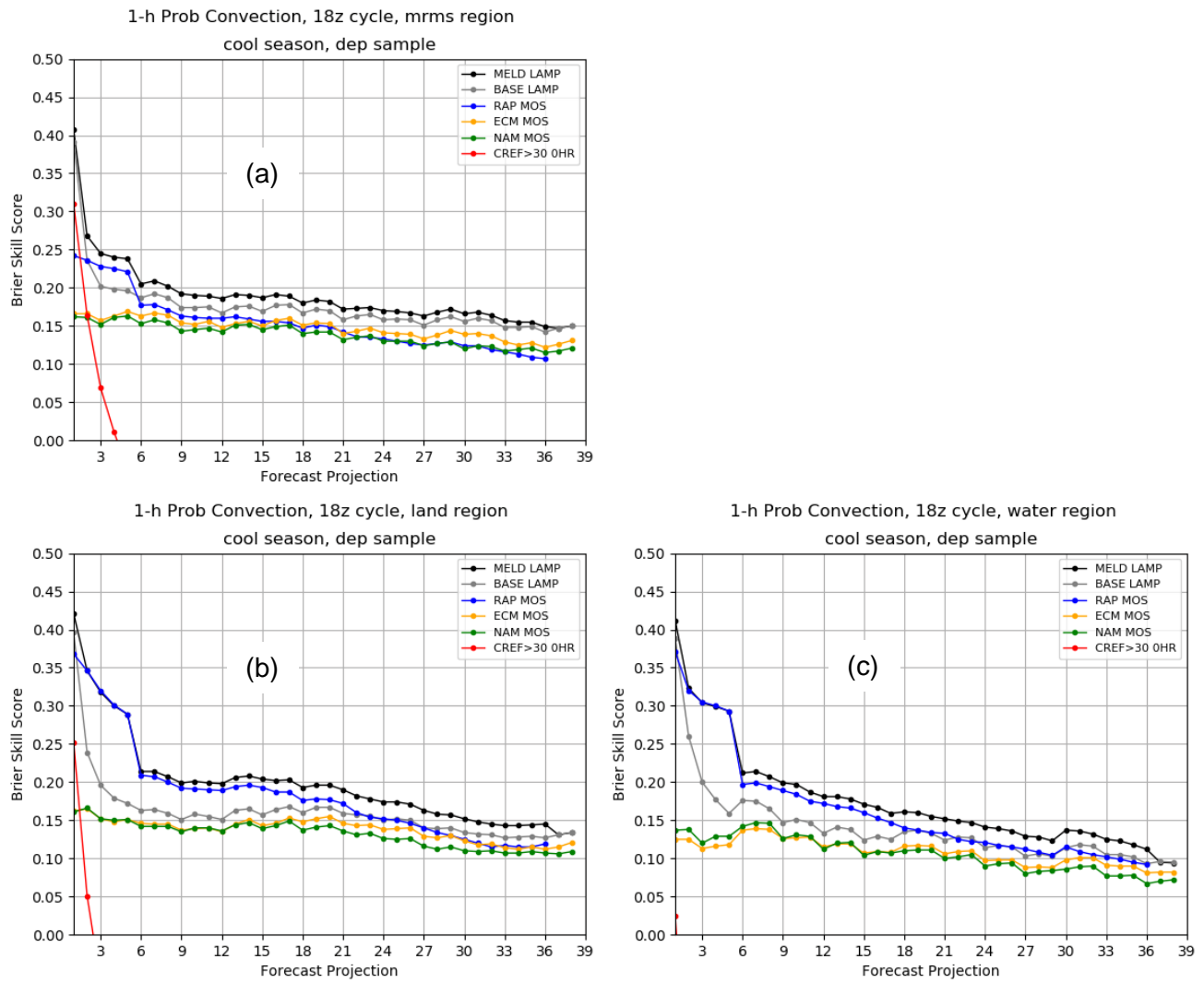


Figure 8. As in Figure 6 for the 18-UTC LAMP cycle.

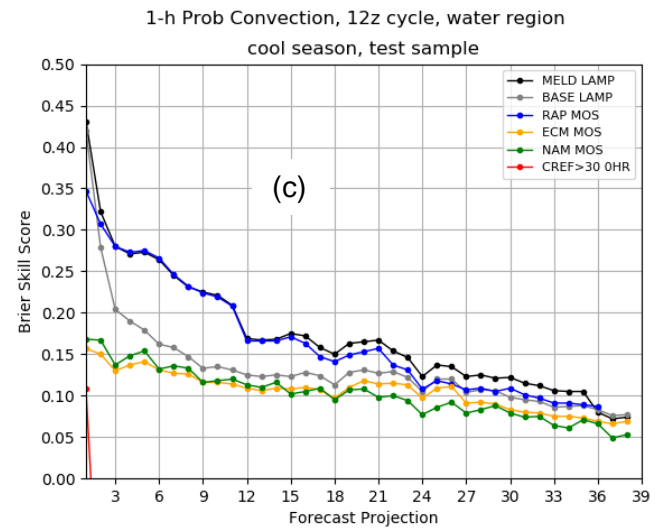
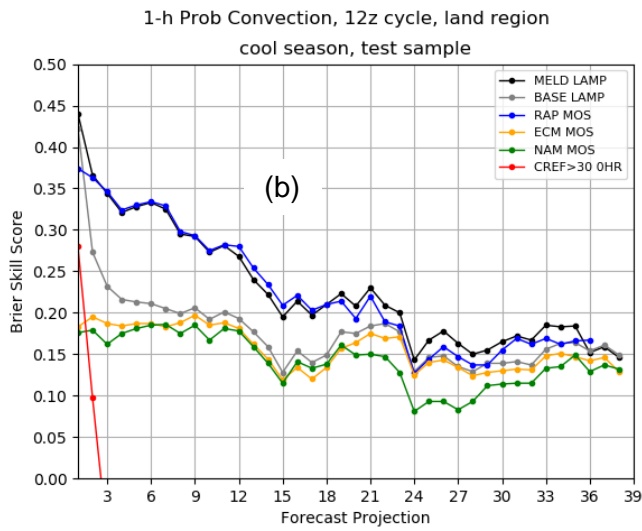
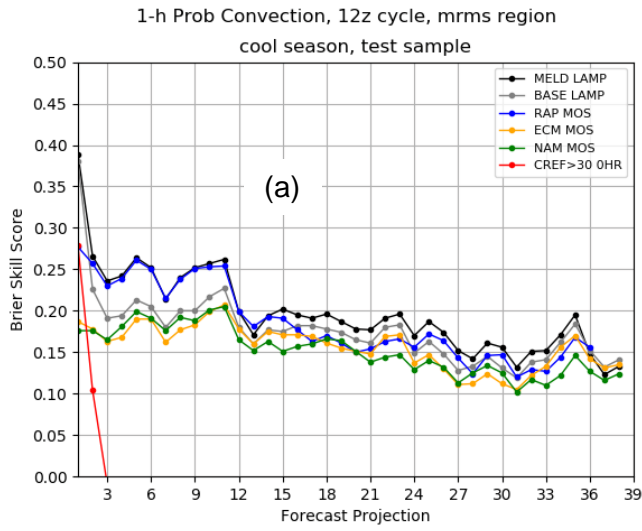


Figure 9. As in Figure 6 for the test sample.

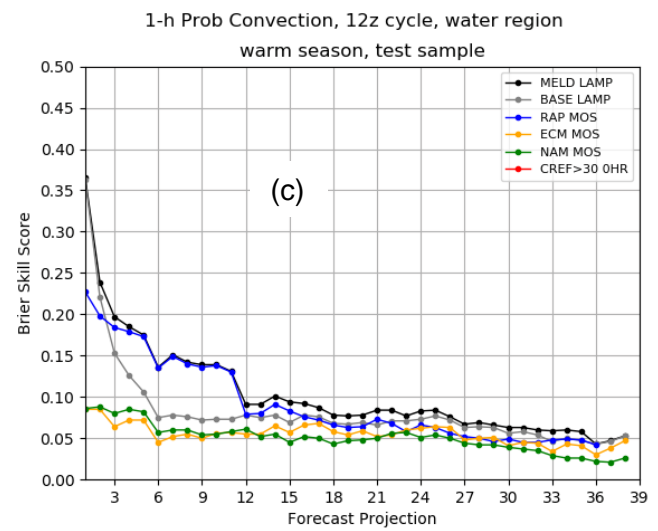
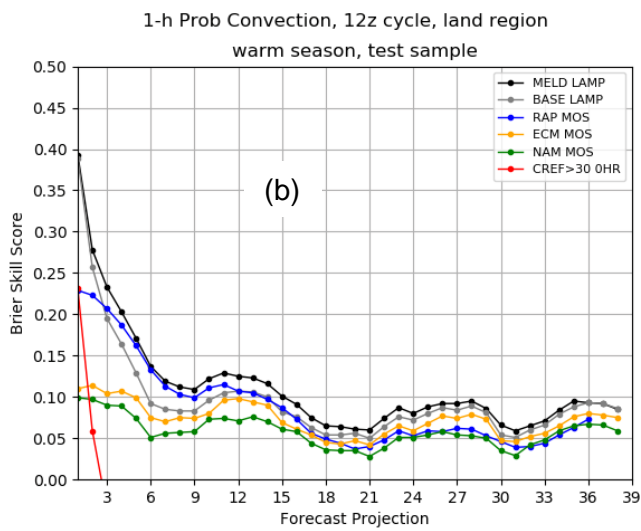
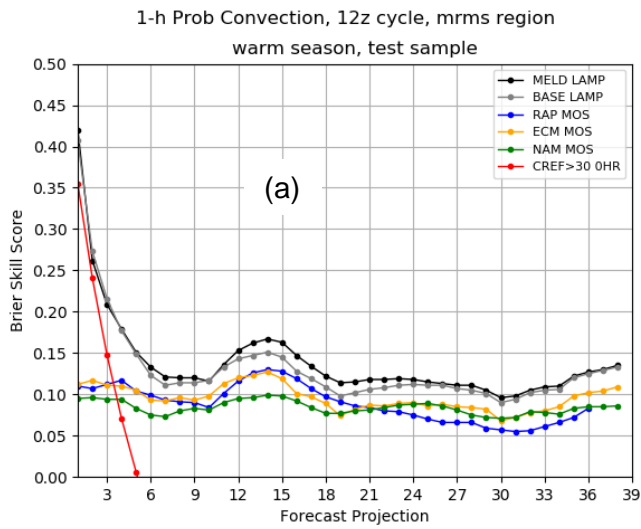


Figure 10. As in Figure 7 for the test sample.

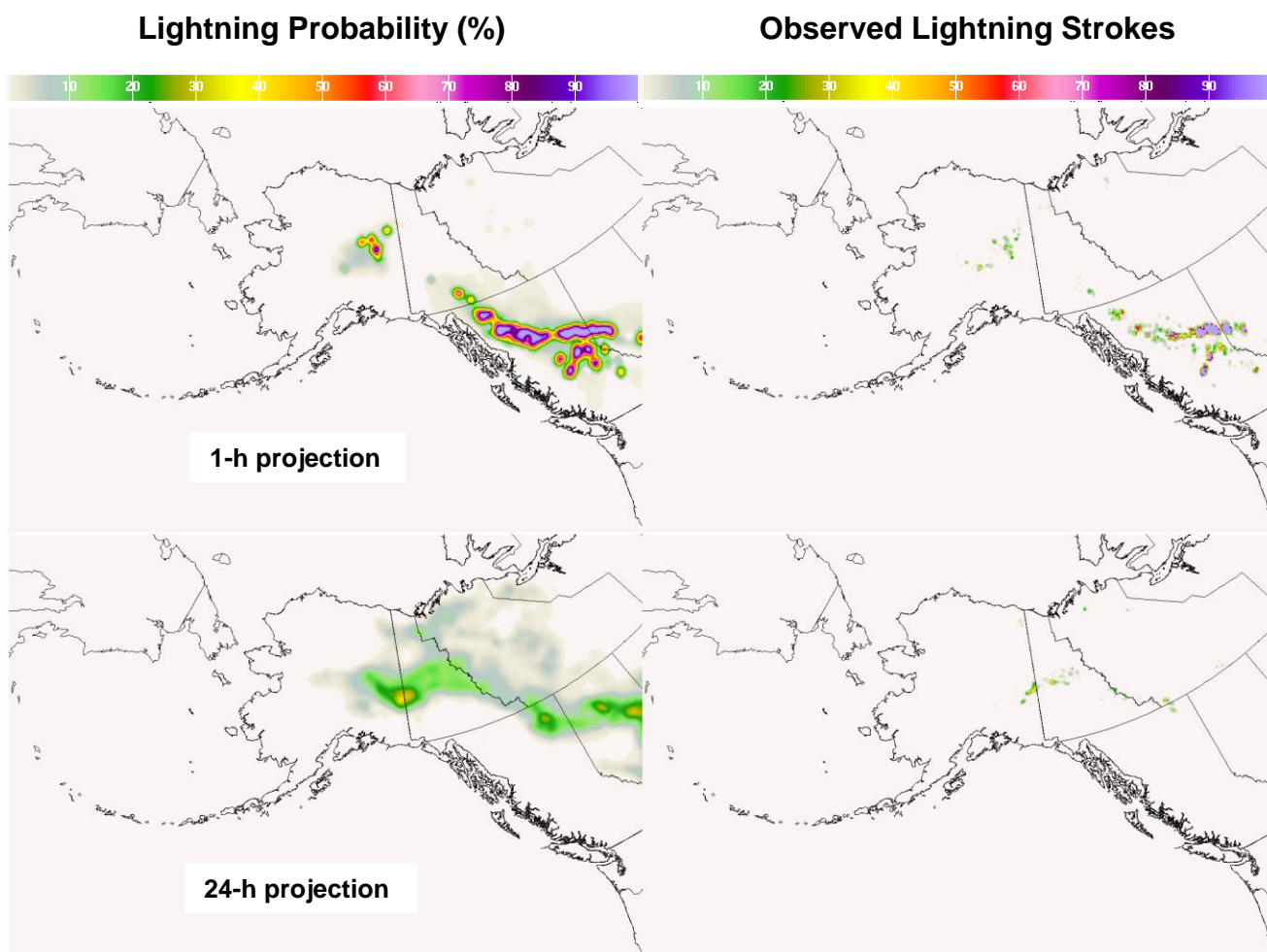


Figure 11. Meld-LAMP lightning probability forecast (left) and verifying, observed cloud-to-ground lightning stroke count (right) for the 1-h projection and the 24-h projection from 00 UTC, 08 July 2017. Note: a verifying lightning event is ≥ 1 strokes.

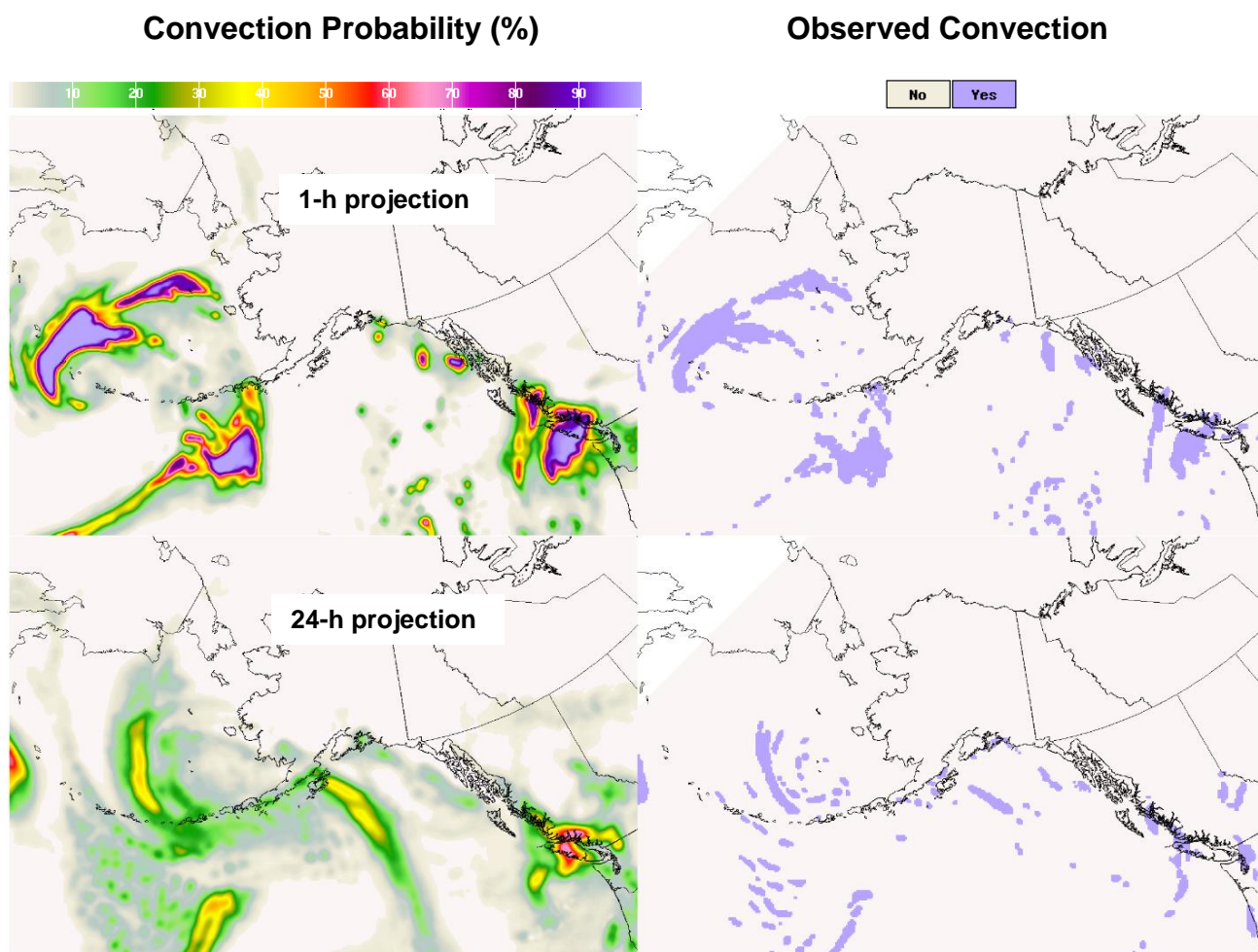


Figure 12. Meld-LAMP convection probability forecast (left) and verifying convection observation (right) for the 1-h projection and the 24-h projection from 00 UTC, 26 November 2017.

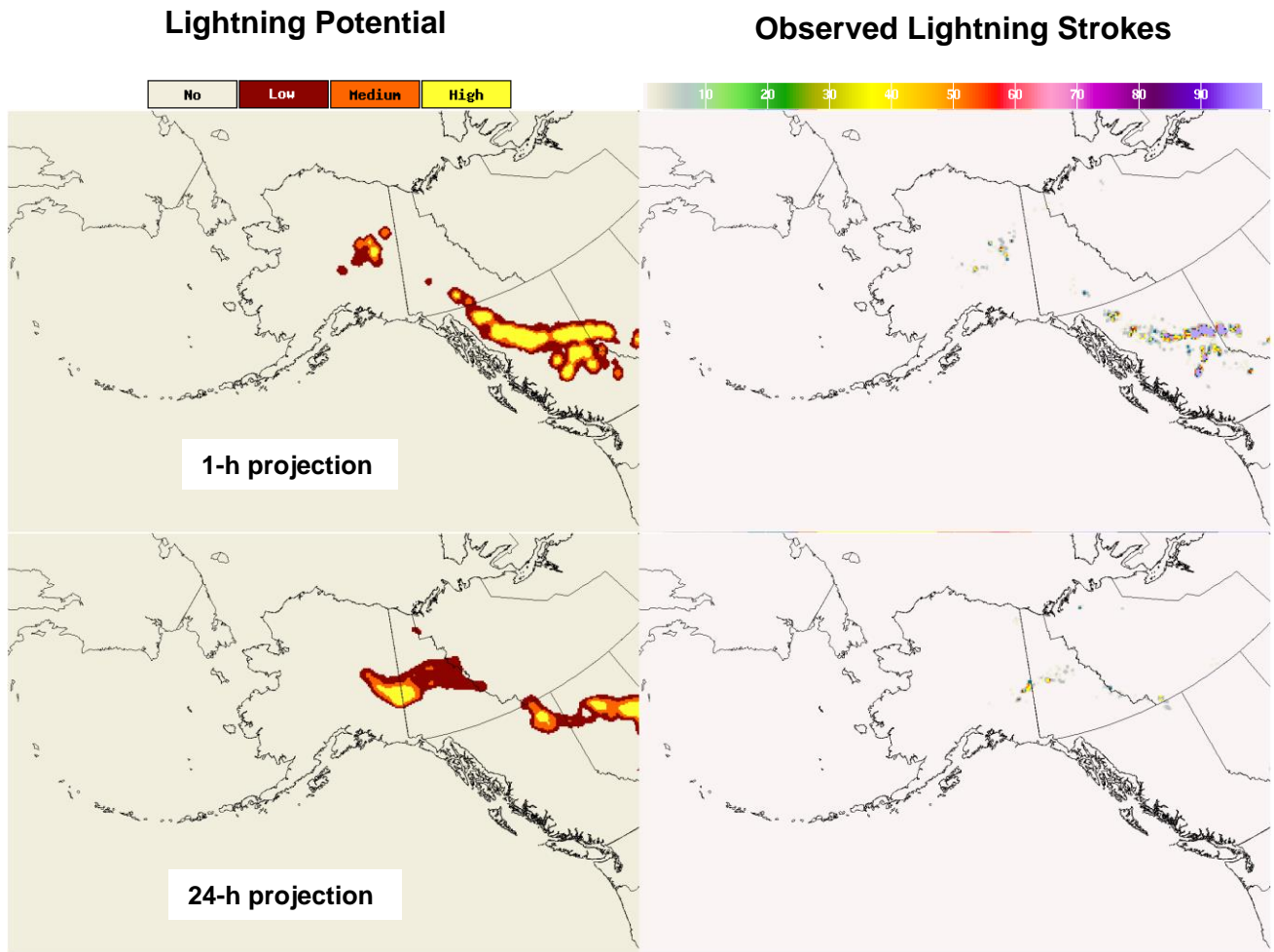


Figure 13. As in Fig. 11 for potential.

Convection Potential

Observed Convection

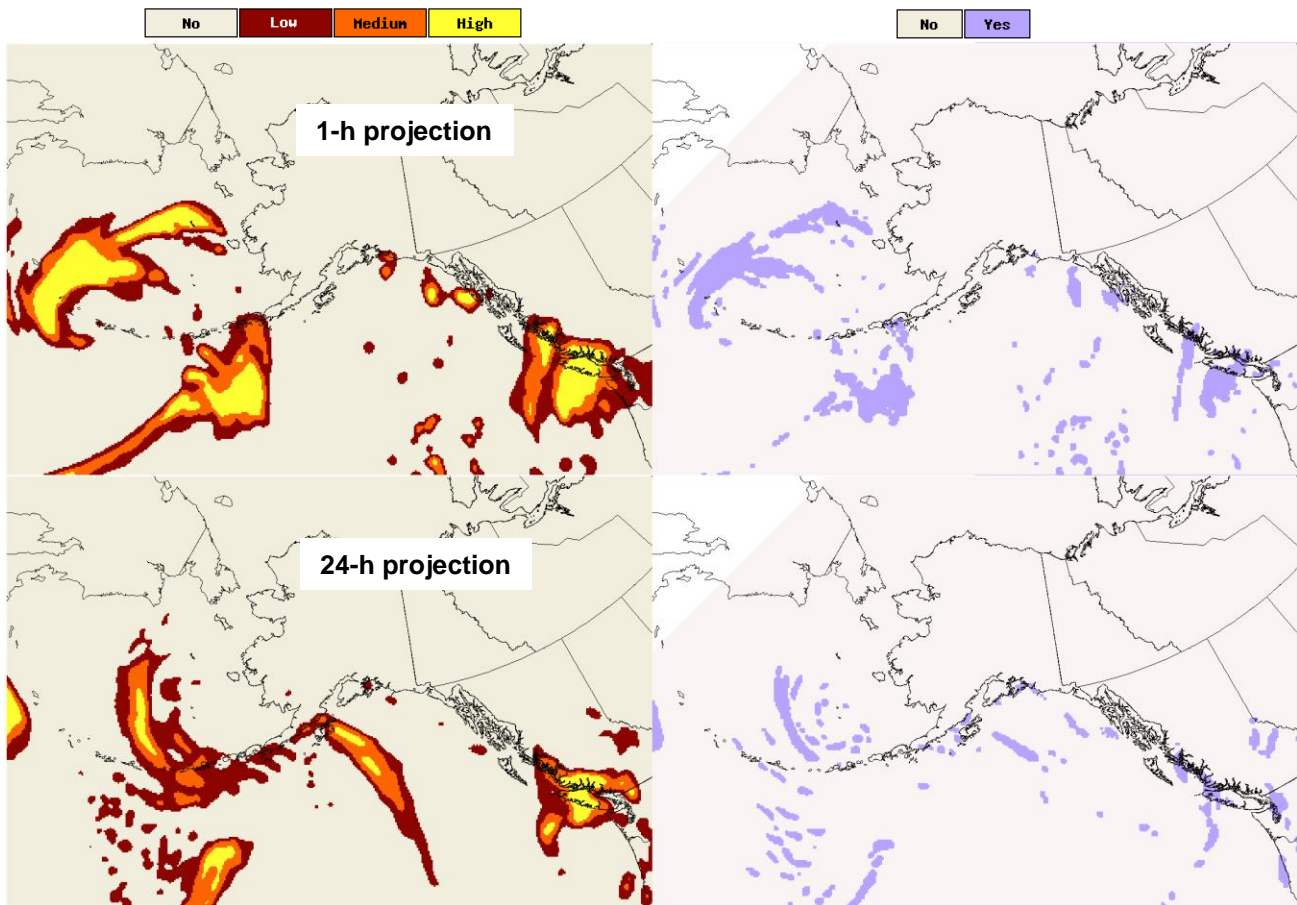


Figure 14. As in Fig. 12 for potential.

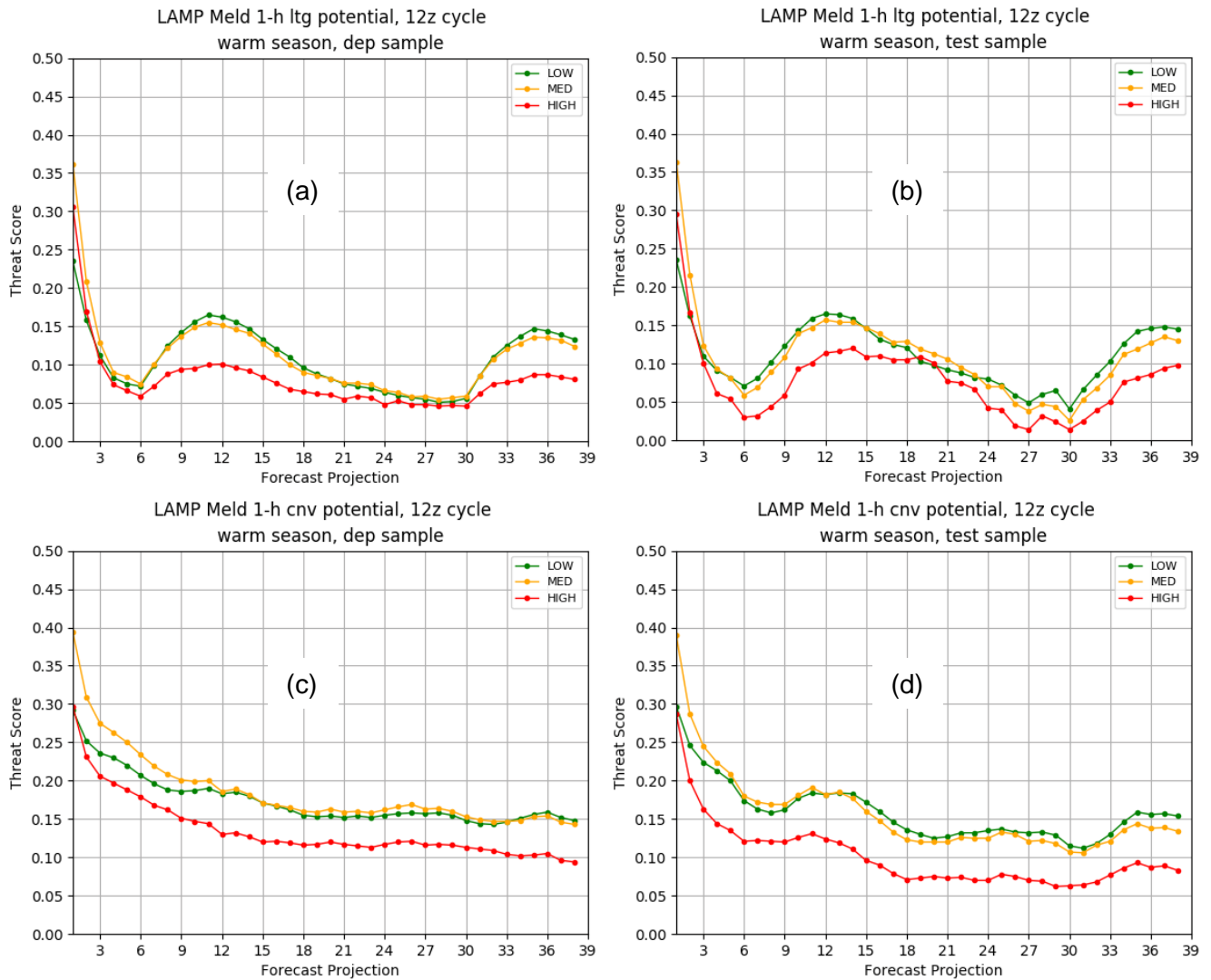


Figure 15. Threat score for meld-LAMP (same as “LAMP Meld” in chart title) lightning potential thresholds for the full NBM grid area, 12-UTC cycle, and the warm season, where (a) is for the developmental sample and (b) is for the test sample; (c) is as in (a) and (d) is as in (b) for convection. Legend items denote potential category thresholds for predicted lightning (or convection) event occurrence: LOW – low and above; MED – medium and above; HIGH – high.

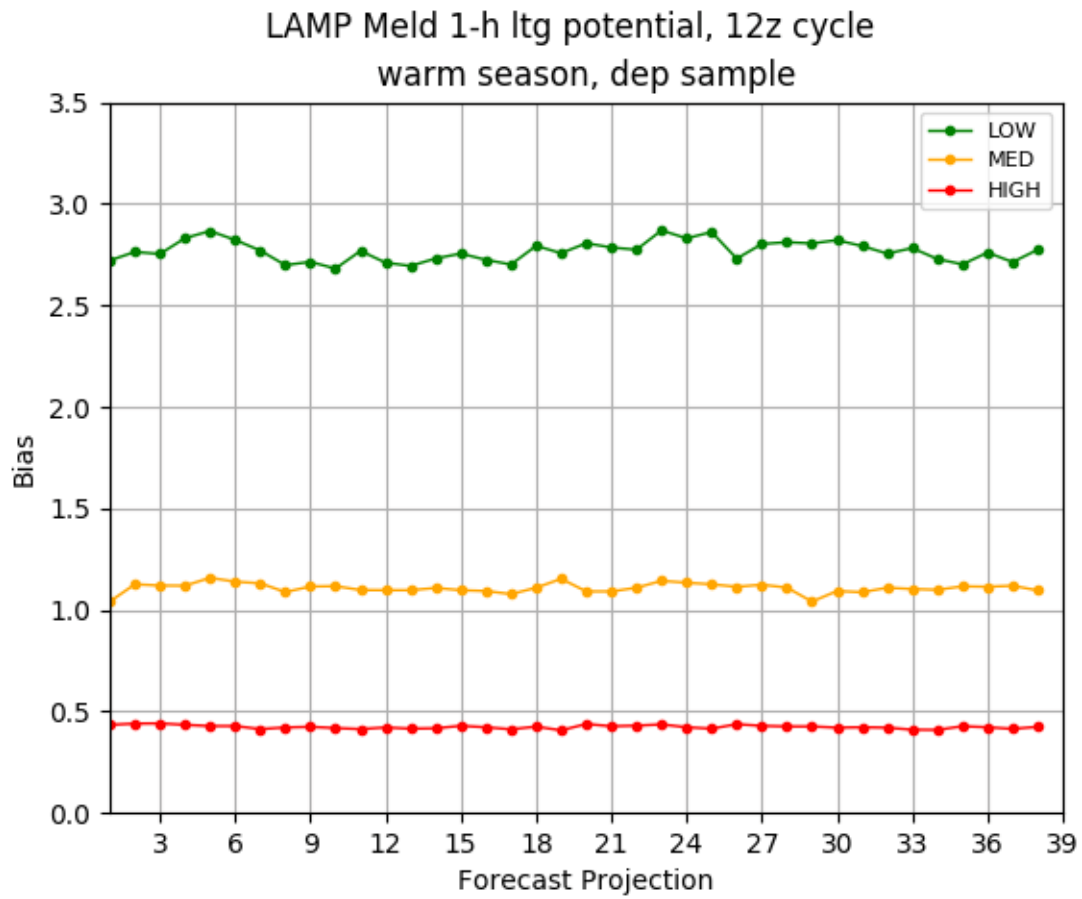


Figure 16. Meld-LAMP (same as “LAMP Meld” in chart title) bias for lightning corresponding to Fig. 15a (12-UTC cycle, warm season, developmental sample).